

See discussions, stats, and author profiles for this publication at: <https://www.researchgate.net/publication/45378992>

Theoretical results on toroidal vesicles

Article in *Journal of Physics B Atomic and Molecular Physics* · September 1992

DOI: 10.1051/jp2:1992229

CITATIONS

24

READS

40

1 author:



Bertrand Gabriel Fourcade
University of Grenoble, France

63 PUBLICATIONS 1,781 CITATIONS

SEE PROFILE



Theoretical results on toroidal vesicles

B. Fourcade

► **To cite this version:**

B. Fourcade. Theoretical results on toroidal vesicles. Journal de Physique II, EDP Sciences, 1992, 2 (9), pp.1705-1724. <10.1051/jp2:1992229>. <jpa-00247761>

HAL Id: jpa-00247761

<https://hal.archives-ouvertes.fr/jpa-00247761>

Submitted on 1 Jan 1992

HAL is a multi-disciplinary open access archive for the deposit and dissemination of scientific research documents, whether they are published or not. The documents may come from teaching and research institutions in France or abroad, or from public or private research centers.

L'archive ouverte pluridisciplinaire **HAL**, est destinée au dépôt et à la diffusion de documents scientifiques de niveau recherche, publiés ou non, émanant des établissements d'enseignement et de recherche français ou étrangers, des laboratoires publics ou privés.

Classification

Physics Abstracts

82.70—02.40—68.15

Theoretical results on toroidal vesicles

B. Fourcade

Institut Laue-Langevin, 156 X Grenoble Cedex 38042, France

(Received 4 December 1991, accepted in final form 16 June 1992)

Resumé. — Selon une conjecture due à Willmore [5], la surface torique correspondant au *minimum minimorum* de l'énergie de courbure est soit un tore à symétrie axiale dont le facteur de forme est $\frac{1}{\sqrt{2}}$ soit un de ses transformés conformes. On étudie ce problème dans le contexte d'une vésicule fluide sujette aux contraintes et d'aire constante, (soit un nombre de lipides fixe) et de volume constant (soit aucune perméation au travers de la membrane). En particulier, on montre que les contraintes n'altèrent pas la dégénérescence conforme [7, 8], lorsque la variation normale à la surface est calculée au deuxième ordre. On donne en plus la hiérarchie complète des modes qui brisent sélectivement les deux symétries de ce tore axi-symétrique. Nous montrons que le problème des symétries est clarifié si ces surfaces toriques sont représentées comme des surfaces bi-dimensionnelles plongées dans l'hypersphère de R^4 . De façon générale, on montre qu'une courbure spontanée positive induit une instabilité vers des formes non-axisymétriques où le trou est excentré. S'inspirant du problème des Cyclides de Dupin, on emprunte une approche variationnelle pour calculer le seuil de cette instabilité en fonction du volume réduit. En dernier lieu, nous discutons une série d'expériences que ces calculs peuvent illustrer.

Abstract. — According to a conjecture due to Willmore [5], the toroidal surface corresponding to the *absolute minimum* of the curvature energy is either an axisymmetric torus of aspect ratio $\frac{1}{\sqrt{2}}$ or its conformal transform. We study this problem in the context of a fluid vesicle under the constraints of constant area, i.e. constant number of lipid molecules, and of constant enclosed volume, i.e. no permeation through the membrane. We show, in particular, that, when the calculation is carried out to second order in variations normal to the surface, these constraints do not remove the conformal degeneracy [7, 8]. We give the complete hierarchy of modes which selectively break all the symmetries of a torus. We show that this symmetry problem is clarified if these toroidal surfaces are represented as 2d-dimensional surfaces embedded in the hypersphere of R^4 . Our calculation demonstrates that a positive spontaneous curvature favors non-axisymmetric shapes, where the hole has moved off the center. Inspired by the Dupin Cyclide problem, we provide a variational Ansatz to give the threshold of this non-azimuthal instability as a function of the reduced volume. Finally, we discuss a new set of possible experiments to which our calculation can be applied.

1. Introduction.

When immersed in an aqueous environment, phospholipid molecules spontaneously form a solution of vesicle structures. Under observation, these vesicles exhibit a rich variety of shapes and, until recently, their taxonomy has mainly concentrated on spherical topology, including discocytes, stomatocytes or even budded shapes [1]. In this paper we shall report theoretical results for toroidal vesicles which provide and extend the mathematical basis of our analysis outlined in reference [2]. The experimental motivation is based on the works of Mutz and Bensimon, which showed that such toroidal vesicles are experimentally observable [3]. The following report provides a new set of quantities which could be checked against experiment.

Based on the works of Canham, Helfrich and Evans [4] the shape problem for a vesicle is the minimization of an elastic bending energy for a closed surface at a given area (i.e. fixed number of molecules) and volume (i.e. no permeation through the membrane). Under some circumstances, as we shall discuss later, the latter constraint can be however temporarily released. For vesicles with toroidal topology, the minimization program has been considered both in mathematics [5] and later in physics [6-8]. Ou-Yang Zhong-Cahn showed that the only circular and axisymmetric torus which is a stationary shape corresponds to two generating circles with ratio $1/\sqrt{2}$, the so-called Clifford torus. The main result of this calculation is to show that this torus is still a stationary solution of the shape problem with a non-zero spontaneous curvature. For zero spontaneous curvature and without constraints, this result is known in mathematics as the Willmore conjecture [5] which states that, up to a conformal transformation, the *minimum minimorum* of the curvature energy for genus one surfaces corresponds to this torus. As recalled by Duplantier [7], the bending elastic energy is a conformal invariant so that this absolute minimum is indeed degenerate. The experimental consequence is that non-axisymmetric shapes, conformal transforms of the axisymmetric torus, are also minimum of the bending energy, so that they are experimentally accessible. As stated in this reference, a spontaneous curvature term breaks this degeneracy, but for small spontaneous curvature it is likely that observable shapes are the almost conformal transformed of the Clifford torus. This was the point developed in reference [1] with respect to experimental observations, where an almost conformal transformed torus was shown to be experimentally observable. Finally, Seifert [8] studied numerically the axisymmetric shape problem for toroidal vesicle subject to both constraints of constant area and constant volume. As a result of these constraints, there are families of axisymmetric tori that are stationary solutions of the problem. They are organized as different branches of a non-circular meridian cross-section, whose energies depend on the reduced volume. This author [8, 9] also made use of conformal transformations to show that a positive spontaneous curvature makes a series of these branches unstable with respect to a shift of the hole. We shall however point out that, in the case of the Clifford torus, there is only one unstable branch corresponding to only one almost conformal mode.

In this paper, we shall concentrate on the Clifford torus or on its conformal transformed. Motivated by experimental observations, we think that it is valuable to provide an analytical study as complete as possible of simple objects endowed with a rich and experimentally accessible variety. Some of the following results can be directly compared with experimental data (See, for example, Figs. 5 together with Eq. (25)).

To this end, we first make contact with the point of view of modern Differential Geometry where surfaces which make the bending action extremal are described as stereographic projection images of surfaces embedded in the unit hypersphere of a four-dimensional space. From a physical point of view, this approach gives a powerful tool to provide non-trivial examples of high genus surfaces [10]. It also clarifies the hierarchy of symmetries, which are selectively broken by each fluctuation mode. Our discussion follows Peterson's approach [11] for the quasi-

spherical problem and we shall concentrate on two different statistical ensembles: the constant area and constant volume ensemble or the constant area and constant pressure ensemble. The result is that a positive spontaneous curvature [12] makes the Clifford torus unstable with respect to a shift of the hole. This point has been previously addressed by Ou-Yang Zhong-Chan [6] and Seifert, [8] but the following discussion is more complete. As a following point, we illustrate the non-axisymmetric problem in Chapter IV. We take a variational approach which is justified in the case of a small spontaneous curvature. Our trial shapes are surfaces for which the principal lines of curvature are circles. This is equivalent to the problem of Dupin Cyclides or confocal conics [13] which give a generic model to describe the organization of defects in liquid crystals [14]. The physical consequences of this calculation can be found in subsection B. We discuss these results with respect to experimental observations where an instability towards non-axisymmetric shapes may be driven by changing the osmotic pressure. Using this variational calculation, we suggest some experiments for the non-axisymmetric shape problem. Finally, the conclusion sums up our findings.

2. The Clifford Torus as a surface in S^3 .

To understand closed 2D surfaces minimizing the bending energy in the physical 3D space, it may be easier to consider them as stereographic projections of 2D surfaces but embedded in the hypersphere of the 4 dimensional space. The reason for this is that curvature terms are more easily computed for surfaces embedded in S^3 than for their stereographic R^3 image. This procedure makes also clear the symmetries which are selectively broken when the 3D vesicle fluctuates around its equilibrium shape. Since a stereographic projection is a conformal mapping, there is an invariant which gives the bending energy in the 3D space. Let H and K be the mean curvature and the Gaussian curvature *relative* to S^3 . We know that [5]

$$\frac{1}{2} \int dS_{S^3} (H^2 - K) = \frac{1}{2} \int dS_{R^3} (H^2 - K), \quad (1)$$

where the right-hand side of equation (1) is the pure bending energy, since the Gaussian curvature term is a topological invariant [15]. This point of view is best illustrated in the case of circular toroidal shapes of genus zero where algebraic manipulations are fairly easy. The points we want to illustrate are :i) the Clifford torus is a minimal surface in S^3 associated with a stationary shape in R^3 for the pure bending problem; ii) all variations with respect to the normal are in one-to-one correspondence between the two spaces. The first point is not new but the connection with minimal surfaces in S^3 is crucial for giving examples of high genus surfaces which minimize the curvature energy in R^3 [10]. From our point of view, this procedure simplifies the algebra for the second variation of the bending energy with the area-volume constraints [16].

Let us consider S^3 as the set of points for which $\sum_{i=1}^{i=4} x_i^2 = 1$. If we decide that

$$(x_1 = 1; x_{2,3,4} = 0),$$

represents the north pole, we associate to each point of the hypersphere its stereographic projection (x, y, z) in R^3 as

$$x = x_3/(1 - x_1); y = x_4/(1 - x_1); z = x_2/(1 - x_1). \quad (2)$$

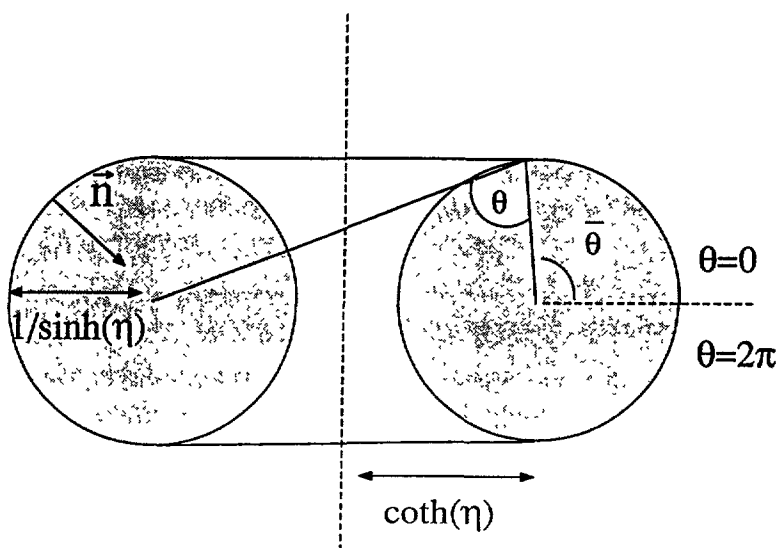


Fig.1. — System of toroidal: coordinates the angle θ is defined with respect to the largest generating circle of radius $R = a \coth(\eta)$, the other circle having a radius of $1/\sinh(\eta)$. The angle $\bar{\theta}$ corresponds to the usual angle in a cylindrical coordinate system. The mathematical formula relating both systems can be found in Appendix A.

By definition, spherical tori in S^3 are $\psi = \text{cst.}$ surfaces for which we have

$$x_1 = \sin(\theta) \sin(\psi); x_2 = \cos(\theta) \sin(\psi); x_3 = \cos(\phi) \cos(\psi); x_4 = \sin(\phi) \cos(\psi). \quad (3)$$

The stereographic projection maps each of these tori onto an axisymmetric circular toroidal surface of R^3 . By definition, a circular torus has two circular meridian cross-sections. If one takes an arbitrary point on the hypersphere as the apex of the stereographic projection [16], the projected shape is a non-axisymmetric torus where the hole has moved off the center (see the Dupin Cyclide section).

The usual toroidal coordinate system used, for example, in reference [6] is defined as (η, θ, ϕ) with $\cosh(\eta) = 1/\sin(\psi)$, where ϕ is the azimuthal angle and θ is defined with respect to the largest generating circle (See Fig. 1 for geometric definitions). The aspect ratio of the torus is given by the ratio of the two generating circles, $\cosh(\eta)$, which is $\sqrt{2}$ for the Clifford torus (See Fig. 1 and Appendix A for more mathematical details).

For a $\psi = \text{cst.}$ torus in S^3 , we find that the metric tensor is diagonal with $g_{\theta,\theta} = (\sin(\psi))^2$ and $g_{\phi,\phi} = (\cos(\psi))^2$. In this representation we can define the curvature tensor from the variation of the vector \mathbf{n} , normal to the torus, but *tangent* to S^3 . In the coordinate representation of equation (3), this vector is

$$\mathbf{n} = (\cos(\psi) \sin(\theta), \cos(\psi) \cos(\theta), -\sin(\psi) \sin(\phi), -\sin(\psi) \cos(\phi)).$$

The curvature tensor relative to S^3 is defined by $\partial_i \mathbf{n} = h_{i,j} \mathbf{t}_j$ where $\partial_\theta \mathbf{OM} = \mathbf{t}_\theta$, $\partial_\phi \mathbf{OM} = \mathbf{t}_\phi$. As a result, for the family of $\psi = \text{cst.}$ circular tori, one finds $h_{\theta,\theta} = \cot(\psi)$ and $h_{\phi,\phi} = -\tan(\psi)$. The $\psi = \pi/4$ torus is, therefore, a minimal surface of zero mean curvature $H = 1/2(h_{\theta,\theta} + h_{\phi,\phi})$ and has a constant Gaussian curvature $K = -1$. Its bending energy can be calculated as

$$\frac{1}{2} \int dS_{S^3} (H^2 - K) = \frac{\pi^2}{2 \cos(\phi) \sin(\phi)} = \pi^2 \frac{\cosh(\eta)^2}{2 \sinh(\eta)} = \frac{1}{2} \int dS_{R^3} (H^2 - K), \quad (4)$$

where we have used that the Gaussian curvature term of a torus in R^3 is zero [17]. The last equality can be checked in R^3 using the toroidal coordinate system of figure 1 and of Appendix A.

From equation (4), it is easy to show that the circular torus which minimizes the curvature energy corresponds to $\psi = \pi/4$. This is the Clifford torus. To study the second variation of curvature elastic energy in R^3 , we first consider normal variations in S^3 and use a stereographic projection from the north pole to get the corresponding variations in R^3 .

For a ψ axisymmetric torus of circular cross-section the eigen-modes of the second variations are associated with two classes of symmetry breaking terms. The first hierarchy breaks the circular meridian cross-section and it is associated with a variation (u_n, v_n) along the normal in S^3 as

$$\psi(\theta) = \pi/4 + \sum_{n=0}^{\infty} u_n \cos(n\theta) + v_n \sin(n\theta). \quad (5)$$

In the same way, the azimuthal symmetry is broken for a variation along the normal to the surface. It suffices to take ψ as a function of ϕ , as in equation (5) with θ replaced by ϕ . Because of symmetry reasons, both variations lead to the same variation for the bending Hamiltonian and one finds

$$\delta \left(\frac{2}{\pi^2} \int dS_{S^3} (H^2 - K) \right) = \sum_0^{\infty} \frac{1}{2} (u_n^2 + v_n^2) (2 - 3n^2 + n^4), \quad (6)$$

where u_n, v_n are the Fourier components of ψ in θ , or in ϕ . As a result of equation (6), the corresponding R^3 hierarchy, $\delta\eta(\theta, \psi) = -\sqrt{2} \delta\psi(\theta, \phi)$, gives a complete set of eigen-modes for the curvature elastic energy. To conform ourselves with the toroidal coordinate system, the normal of the R^3 torus is chosen to point inwards the surface. With this convention, $\eta \rightarrow \eta + \delta\eta$ amounts to making a variation normal to the surface, $M \rightarrow N$, such that

$$MN = -\frac{\delta\eta(\theta, \phi)}{\cosh(\eta) - \cos(\theta)} \mathbf{n}, \quad (7)$$

where the metric tensor of Appendix A gives the surface and the volume of the perturbed Clifford torus. For simplicity, we shall write $a_n = -\sqrt{2}u_n$; $b_n = -\sqrt{2}v_n$ for the Fourier components of $\delta\psi$. For an azimuthal variation, we have directly checked in R^3 that equation (6) gives the correct variation. The set of $n = 1$ modes gives the complete set of conformal modes, since from equations (1) and (6), they are zero energy modes.

When dealing with the vesicle problem, this set of eigenvectors cannot, however, describe the short time scale fluctuations around the Clifford equilibrium shape since both surface and volume must be conserved [11]. These constraints restrict the variation space accessible to the system and this is now defined by a mode coupling approach.

3. Fluctuations around the Clifford torus.

We shall first concentrate on fluctuations which conserve both area and volume and we shall consider thereafter a configuration space where area and pressure are kept constant. Because there are an arbitrary number of ways to couple each eigenvector to assure both surface and

volume conservation, the mode coupling approach is not uniquely defined. We shall concentrate on a minimal coupling approach which gives the lowest energy eigenstates for the appropriate configuration space. The procedure is to couple to all the eigen-vectors of the preceding section two "slave" modes in order to satisfy the constraints. The configuration space has, therefore, a co-dimension two.

The first eigen-vector corresponds to a *breathing* deformation with $\delta\eta = cst$ where the radius of the largest generating circle, $R = \coth(\eta)$, and of the smallest one, $r = 1/\sinh(\eta)$, have opposite variations as a function of η (See Fig. 1). This breathing deformation does not break the symmetries of the circular axisymmetric torus but it only changes its aspect ratio (and its reduced volume). The second eigenvector chosen in order to satisfy the constraints is a global rescaling. For a bare bending energy, the latter is a zero mode energy and, in the θ representation of the preceding section, this is equivalent to choosing $\delta\eta(\theta) = b_1 \cos(\theta)$. In this parametrization, all lengths are scaled by a factor $1 - b_1$. Let us mention that the corresponding $n = 1$ even term, $\delta\eta(\theta) = b_1 \sin(\theta)$, gives a translation along the azimuthal symmetry axis and it can be discarded.

3.1 THE ZERO-SPONTANEOUS CURVATURE CASE. — Let us first consider the case where the azimuthal symmetry is broken. Because of symmetry reasons, we can restrict our study to variations of the type $\delta\psi(\phi) = a_n \cos(n\phi)$ with a volume and area given by $(\cosh(\eta_0) = \sqrt{2})$

$$S = 4\pi^2 \frac{\cosh(\eta_0)}{\sinh(\eta_0)^2} \left(1 + \frac{a_n^2}{4}(7 + n^2)\right), \quad (8)$$

$$V = 2\pi^2 \frac{\cosh(\eta_0)}{\sinh(\eta_0)^3} (1 + 4a_n^2). \quad (9)$$

As a result, to keep the surface and volume constant to second order in the normal variation, we choose to write

$$\begin{aligned} \delta\eta_{0,n} &= a_n \cos(n\phi) + a_0 + b_1 \cos(\theta), \\ a_0 &= \frac{\sqrt{2}}{4} (11 - 3n^2) a_n^2, \\ b_1 &= \frac{\sqrt{2}}{4} (13 - 5n^2) a_n^2, \end{aligned} \quad (10)$$

and the set $\delta\eta_{m,0}(\phi, \theta)_{n \geq 1,0}$ spans the configuration space for azimuthal symmetry breaking variations which conserve both area and volume. The energy associated with each eigenvector is derived from equation (6) as

$$\delta \left(\frac{2E(\eta_{n,0})}{\pi^2} \right) = \sum_1^\infty \frac{1}{4} a_n^2 (2 - 3n^2 + n^4), \quad (11)$$

and, to second order, the constraints do not change the spectrum since they appear as fourth order terms in a_n . Figure 2 shows how the first three $\delta\eta_{n,0}(\phi)$ modes break the azimuthal symmetry: $n = 1$ moves the hole off the center but it keeps its circular shape. For an $n = 1$ mode and to first order in variation normal to the surface, the principal lines of curvature are circles (see the Dupin cyclide section). For $n \geq 2$, the symmetry is of order n , $n = 2$ being an ellipse and $n = 3$ being a star.

Breaking the symmetry of the circular meridian cross-section can be handled in a similar way but, in that case, the constraints remove the degeneracy between the odd and even θ -variations,

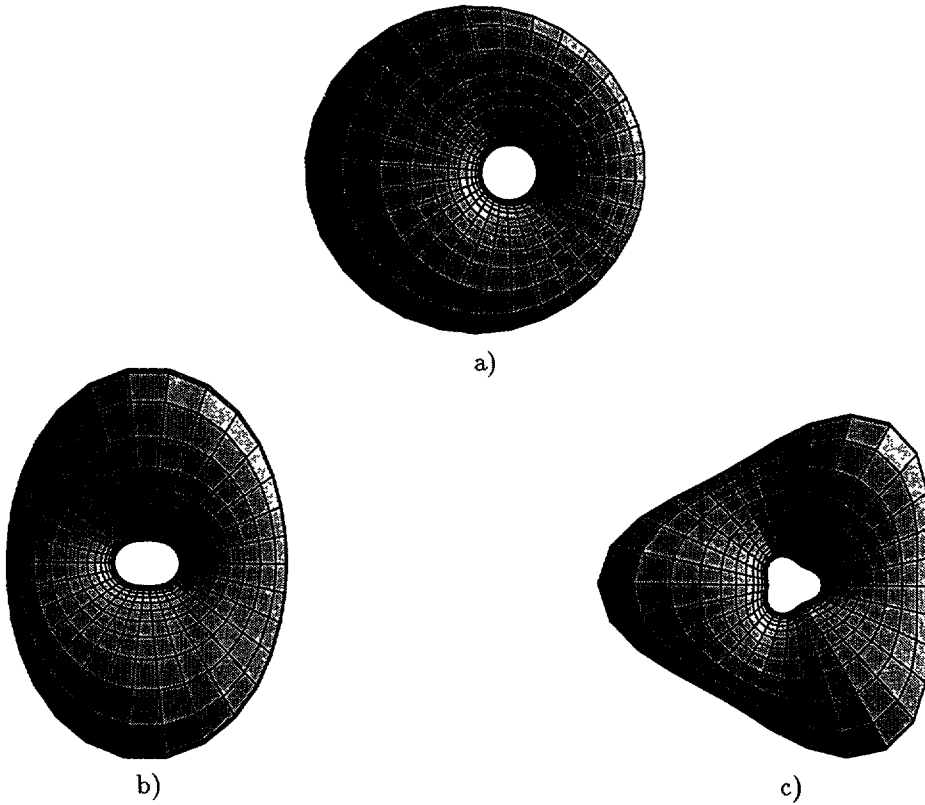


Fig.2. — The first three azimuthal symmetry breaking modes $\delta\eta_{n,0}(\phi) = a_n \cos(n\phi)$, $n = 1, 2, 3$ with $a_n = 0.2$ (Figs. 2a, 2b, 2c, respectively). To linear order in the hole eccentricity, the $n = 1$ shape corresponds to a conformal transformation, whose center of inversion is located on the center of the hole.

i.e. $E(\eta_{0,n,e} = \eta_0 + b_n \cos(n\theta)) \neq E(\eta_{0,n,o} = \eta_0 + b_n \sin(n\theta))$ in equation (6), the energy of the even variations being shifted upwards (See Eqs. (15) and (16)). To see this, first consider the even variations. Since the metric of an unperturbed circular torus is an even function of the toroidal angle θ (see Appendix A), the volume and surface of the perturbed shape changes to *first* order in b_n . As before, one has to couple the $\psi_{0,n,e}(\theta)$ mode with a breathing mode and with a global rescaling to keep area and volume constant. But, in this case, the amplitudes of the slave modes are first order in b_n , so that the amplitude of the breathing mode will shift upwards the energy by an amount proportional to b_n^2 .

Thus, to calculate the spectrum relative to the $\eta_{0,n,e} = b_n \cos(n\theta)$ variation, we need the amplitude of the breathing and rescaling slave mode to first order in b_n . If δS_n and δV_n are the variations of surface and volume associated with $\eta_{0,n,e} = b_n \cos(n\theta)$, we write for the even variation

$$\delta\eta_{0,n,e} = \eta_0 + b_n \cos(n\theta) + b_1 \cos(\theta) + a_0,$$

$$a_0 = \frac{1}{\pi^2} \left(\frac{3}{4} \delta S_n - \delta V_n \right) + O(b_n^2),$$

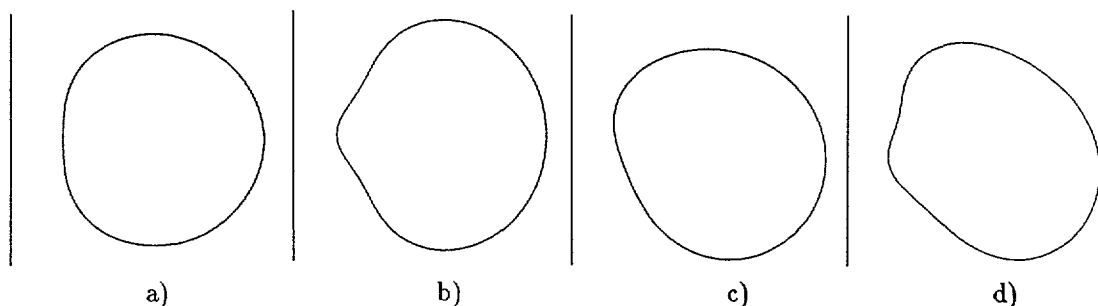


Fig.3. — Meridian cross-section for the first modes which break the circular symmetry of the meridian cross-section: $\delta\eta_{0,n,e}(\theta) = b_n \cos(n\theta)$ (Figs. 3a, 3b), and $\delta\eta_{0,n,e}(\theta) = b_n \sin(n\theta)$ (Figs. 3c, 3d) for $n = 2, 3$ with $b_n = 0.1$. The dark bar corresponds to the azimuthal symmetry axis.

$$b_1 = -\frac{1}{2\sqrt{2}\pi^2} \left(\frac{5}{2} \delta S_n - \delta V_n \right) O(b_n^2), \quad (12)$$

where a_0 and b_1 varies to first order in b_n . Because we want to keep the algebra as simple as possible, let us define the scale invariant reduced volume as

$$v = 3\sqrt{4\pi} \frac{V}{S^{3/2}}, \quad (13)$$

which is equal to 1 for a spherical shape. To counterbalance the change in reduced volume $v_{\text{Clifford}}(1+b_n f(n))$ due to $b_n \cos(n\theta)$, the amplitude of the breathing term $\delta\eta = a_0$ is, therefore, chosen as

$$a_0 = 2\sqrt{2} b_n f(n), \quad (14)$$

which contributes to the $\delta\psi_{0,n,e}$ mode energy by an amount of $16 b_n^2 f(n)^2$ with $f(n=1) = 0.0$, $f(n=2) = 0.18198$, $f(n=3) = 0.20101$.

To compare this result with the odd terms, $\delta\psi_{0,n,o} = b_n \sin(n\theta)$, we note that the amplitude of the breathing deformation necessary to satisfy the constraints is second order in b_n so that, to the same order for the curvature energy, the result does not change from the unconstrained case.

We can summarize as

$$\delta \left(\frac{2E(\eta_{0,n,o})}{\pi^2} \right) = \sum_2^\infty \frac{1}{4} b_n^2 (2 - 3n^2 + n^4), \quad (15)$$

$$\delta \left(\frac{2E(\eta_{0,n,e})}{\pi^2} \right) = \sum_2^\infty \frac{1}{4} b_n^2 (2 - 3n^2 + n^4) + 16 f(n)^2 b_n^2, \quad (16)$$

Figure 3 shows how the first $\delta\eta_{0,n}$ modes break the circular meridian cross-section. As usual, the cosine modes, which conserve the upside-down symmetry, give a lower excitation branch than the odd sinus modes.

As expected from the Willmore conjecture, the stability analysis of this section has shown that this shape is indeed a stable minimum curvature energy shape. To second order in the deformation, the constraints of constant volume and area do not remove the conformal

degeneracy. To see this, we consider $\delta\psi_{1,0,e}$ or $\delta\psi_{0,1,o}$. From equations (11) and (14), these deformations cost no energy and they are akin to Goldstone modes [18]. However, there is only one non-trivial branch, since the mode associated with the θ variation corresponds to a simple rescaling.

3.2 THE NON-ZERO SPONTANEOUS CURVATURE CASE. — According to Helfrich [4], the shape of a vesicle is controlled by a bending elastic Hamiltonian where the inside-outside symmetry can be broken by a spontaneous curvature. This heuristic term has a microscopic origin, e.g. the two sides of the membrane may be in contact with different environments [19], and we shall hereafter assume that the bending term is modified as

$$E = \frac{1}{2} \int dS (H - c_0)^2 \quad (17)$$

Ou-Yang Zhong Cahn has shown that the Clifford torus is still a relative extremum of the bending elasticity *with both* constraints. Let us remark that this result does not hold if there is only one constraint, area or volume. This can be shown from a linear stability analysis restricted to circular tori. Moreover, a spontaneous curvature term breaks the conformal invariance [7], and the bending energy in S^3 and in R^3 are no more equivalent, so that we derive the calculation in R^3 . As before, we consider the stability from the point of view of symmetries and we first study the azimuthal case.

To second order in $\delta\psi(\phi)$, the mean curvature of the perturbed Clifford torus is given by

$$H = \left(1 - \frac{1}{2} \left(\frac{d\eta}{d\phi}\right)^2\right) H_o(\eta) + \frac{1}{2} \frac{\cosh(\eta) - \cos(\theta)}{\sinh(\eta)} \frac{d}{d\phi} \left[\frac{1}{\sinh(\eta)} \frac{d\eta}{d\phi} \right], \quad (18)$$

where

$$H_o(\eta) = \frac{1}{2} \left((\cosh(\eta) \cos(\theta) - 1) / \sinh(\eta) + \sinh(\eta) \right), \quad (19)$$

gives the mean curvature when η is constant (circular torus case). To conserve both area and volume, we use the same mode coupling approach as before. As a result, for $\delta\psi_{n,0}(\phi)$ given by equation (10), one finds (see Appendix A for some mathematical details)

$$\delta \left(\frac{2E}{\pi^2} \right) = -\frac{3}{2} a_n^2 n^2 + \frac{1}{2} a_n^2 n^4 + (1 - 4c_0\sqrt{2}) a_n^2, \quad (20)$$

and the Clifford torus is unstable with respect to the $n = 1$ mode for any positive spontaneous curvature. As c_0 increases, the $n \geq 2$ components lead successively to an instability.

To understand why the $n = 1$ mode is unstable, let us consider figure 4 where we have applied a $n = 1$ variation to the Clifford torus. The torus has been cut into two parts. The outside shell of figure 4a corresponds to the region where the mean curvature is positive and the inside domain, drawn in part b, is the region where the mean curvature is negative. For an $n = 1$ mode, the hole moves off the center and shrinks. As a result, the fraction of surface with a negative mean curvature decreases and, for a positive spontaneous curvature, the energy decreases.

The stability analysis cannot be trivially extended for fluctuations which conserve the azimuthal symmetry. In the case of a finite spontaneous curvature, the set of $\delta\eta_{0,n}(\theta)$ is no more a basis of eigenvectors. However, for small spontaneous curvature, the Clifford torus is necessarily *stable* with respect to these directions, since the first non-trivial mode, $n = 2$, has a *gap* for $c_0 = 0$. A first order perturbation expansion shows, moreover, that this gap decreases when the spontaneous curvature is positive, so that one expects the Clifford torus to

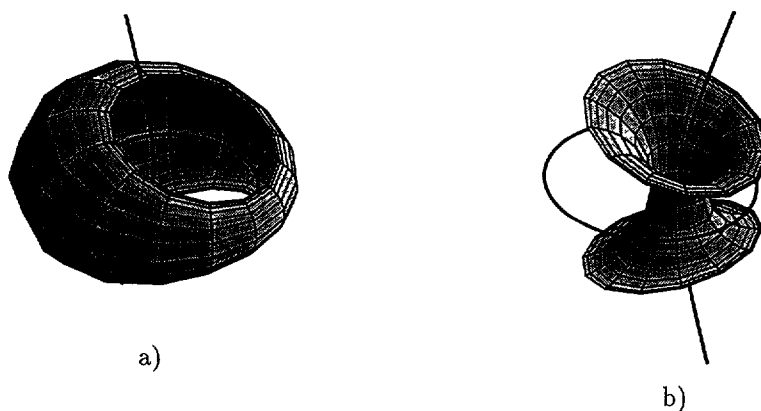


Fig.4. — The two leaves of a non-axisymmetric torus. Part a corresponds to the leaf surrounding the hole, where the mean curvature is negative. Part b gives the outside leaf, where the mean curvature is positive. This shape is a Dupin Cyclide and, to first order in the normal variation, it corresponds to the $\delta\eta_{1,0}(\phi) = a_1 \cos(\phi)$ mode. Note that the hole shrinks when it moves off the center. As a result, the mean-mean curvature decreases. The hyperbola and the ellipse give an illustration of the geometrical construction of section 4. The ellipse and the hyperbola are confocal conics, since the apex of the hyperbola corresponds to the focal points of the ellipse. Their eccentricity is e and $1/e$, respectively. For a top view of the shape see figure 5.

be unstable with respect to a meridian symmetry breaking variation for a finite and positive c_0 .

3.3 FLUCTUATIONS AT CONSTANT PRESSURE AND AT CONSTANT AREA. — Peterson [11] pointed out that, due to permeation through the membrane, fluctuations on long time scale should be calculated in a constant pressure-constant area ensemble. In this case, the free energy differs from the curvature energy, since one has to add up a factor pV to the bending energy, where p is the osmotic pressure difference calculated at equilibrium. Although, the mode coupling approach differs from the above analysis, since the configuration space has now a co-dimension 1, a positive spontaneous curvature also makes the Clifford torus unstable with respect to a shift of the hole. Coupling the $\delta\psi_{n,0} = a_n \cos(n\phi)$ mode with a breathing mode or a global rescaling leads exactly to the same variation of the energy $E + pV$ as in equation (11), when p is chosen as its equilibrium value [6], $p = -32c_0$. [20].

When dealing with the modes which break the circular meridian cross-section, the result differs from the constant area - constant volume ensemble. For zero spontaneous curvature, it is always possible to couple the odd modes and even modes with different scale factors, so that they correspond to degenerate levels in the excitation spectrum. However the first non-trivial mode, $n = 2$, has still a gap and a small spontaneous curvature cannot make the Clifford torus unstable with respect to an axi-symmetric variation.

4. A variational Ansatz: the Dupin cyclides problem.

For a positive c_0 , the stability analysis has demonstrated that the Clifford torus is unstable with respect to a mode breaking the azimuthal symmetry. This circular torus is a particular case, since the three possible conformal transformations give one non-trivial branch, corresponding to

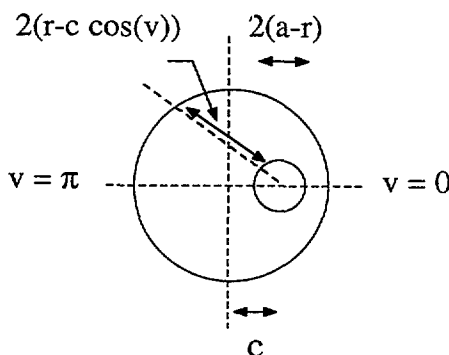


Fig.5. — Top view of a non-axis-symmetric torus with the geometrical definitions used in chapter 4.

the $n = 1$ even mode. It is, therefore, natural to classify non-axisymmetric shapes with respect to the tori which are the conformal transforms of the axisymmetric shapes. The motivation is that, because of symmetry, *all* axisymmetric shapes are necessarily stationary with respect to non-axisymmetric deformations, i.e. their first order energy-variation vanishes. The stability analysis of the previous sections is therefore general and it applies to a whole class of almost circular axisymmetric tori, whose reduced volume differs slightly from the Clifford one.

If one assumes a spontaneous curvature induced, for example, by partial polymerization, the Willmore conjecture is not directly applicable. However, for a small c_0 , one expects the *absolute minimum* to be nearby and we shall address this question with respect to the non-axial stability question. The Clifford torus is, however, the only stationary torus with a circular meridian cross-section and the exact mathematical analysis is difficult in the general case. So we resort to a variational procedure which is shown to reproduce the correct answer within 0.5 % when numerical solutions are possible. The reader uninterested in geometry may skip to section 4.2.

4.1 GEOMETRICAL PRELIMINARIES. — Let us consider circular tori with their conformal transforms. These are the Dupin Cyclides we shall consider as variational shapes. We shall follow the parameterization due to Kléman [14] which allows us to tackle the non-axisymmetric shape problem.

Consider the system of confocal conics of figure 4. If e is the eccentricity of the ellipse, we choose a hyperbola of eccentricity $1/e$, whose apexes are located at the focal points of the ellipse. The class of Dupin Cyclides in which we shall be interested is defined as surfaces for which the centers of curvature are located on these two conics. The geometrical construction we shall use is illustrated in figures 4 and 5, where the parameters can be read off.

Following Kléman [14], we can parameterize the two conics as

$$x_e = a \cos(v) ; y_e = b \sin(v) , \quad (21)$$

for the ellipse, and

$$x_h = c \cosh(u) ; z_h = b \sinh(u) , \quad (22)$$

for the hyperbola. With this parameterization, a and b are half of the ellipse axis and the eccentricity is defined as $e = \frac{c}{a} = \sqrt{1 - \frac{b^2}{a^2}}$.

Let us first concentrate on the inside leaf of the Cyclide, see figure 4b, and let us choose one branch of the hyperbola. The principal lines of curvature are obtained directly from the geometrical construction of the surface. Draw a line between two points of coordinates v , for the ellipse, and u , for the hyperbola. This line intersects the surface at a point M where the two principal spheres of curvature, centered on the ellipse at v and on the hyperbola at u , are tangent at that point. Since the distance between the two centers of curvature is $a \cosh(u) - c \cos(v)$, we define a parameter r such that the radii of the two spheres are $a \cosh(u) - r$ and $r - c \cos(v)$, respectively. Then these two radii are the radii of curvature of the inner leaf.

To obtain the complementary leaf, we consider the other branch of the hyperbola, whose apex is located on the other focal point. As before, the point M is defined as the tangent point of the two spheres but, in this case, the smallest sphere is inside the largest one. This amounts to making the change $r \rightarrow -r$ and one defines the outer leaf, see figure 4a. Then the set (r, a, c) defines uniquely a variational shape, whose meridian cross-section appears as two circles of radii $r - c \cos(v)$ and $r - c \cos(v + \pi)$.

To obtain the metric tensor, we use the arc-length formula $ds^2 = g_{u,u} du^2 + g_{v,v} dv^2$ for any curve drawn on the surface. Let us fix v first. As u varies, the above construction gives a circular sector of radius $\frac{1}{\sigma_1} = r - c \cos(v)$. The rule for similar triangles gives

$$\sigma_1 g_{u,u} du^2 = (dx_h^2 + dy_h^2) \frac{(\sigma_2 - \sigma_1)}{\sigma_1 \sigma_2}, \quad (23)$$

with $1/\sigma_2 = a \cosh(u) - r$. A similar reasoning gives $g_{v,v}$, so that one obtains

$$g_{u,u} = \frac{b^2 \sigma_1^2}{(\sigma_1 - \sigma_2)^2}; \quad g_{v,v} = \frac{b^2 \sigma_2^2}{(\sigma_1 - \sigma_2)^2}. \quad (24)$$

As noted by Kléman [14], there is only one family of cyclides which minimizes the zero spontaneous curvature energy. Using the Euler-Lagrange equations in this coordinate system, $\Delta H + 2H(H^2 - K) = 0$ [21], gives the parameter r as

$$r = \pm \sqrt{a^2 - \frac{b^2}{2}}, \quad (25)$$

where the \pm sign corresponds to the inner or outer leaf, respectively.

The case $a = b$, $r = \frac{a}{\sqrt{2}}$ gives the Clifford torus where the two branches of the hyperbola correspond to the same line giving the azimuthal symmetry axis. When $a = b$ but $r \neq \frac{a}{\sqrt{2}}$, one recovers the breathing mode of the previous section. For $b < a$, the azimuthal symmetry is broken but the shape is a conformal transformed of an axi-symmetric torus. This transformation is an inversion with a center located in the $X - Y$ plane at a distance α from the origin such that

$$\alpha = \frac{ra}{c} \pm \left(\frac{r^2 a^2}{c^2} + c^2 - a^2 - r^2 \right)^{\frac{1}{2}}, \quad (26)$$

and this transformation maps a cyclide onto an axi-symmetric circular torus with two generating circles of ratio

$$R_1/R = \frac{r^2 - c^2}{(r^2 a^2 - c^2(r^2 + a^2 - c^2))^{\frac{1}{2}}}, \quad (27)$$

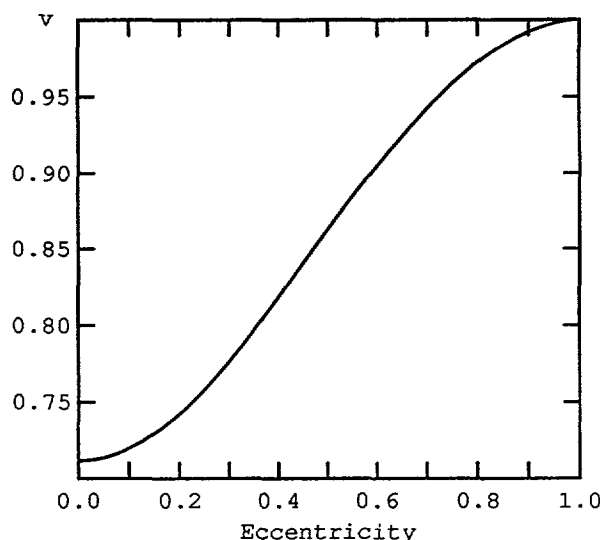


Fig.6. — Reduced volume as a function of the eccentricity for a cyclide which minimizes the *bare* bending energy, i.e. $c_0 = 0$. The axi-symmetric torus has a reduced volume of $v_{\text{clifford}} = 0.711638\dots$

and this is helpful to compute the *bare* energy of any cyclide, since the bending energy is a conformal invariant, see equation (32) below. To keep the algebra as simple as possible, we shall find it useful to define

$$G_1(x) = F\left(\frac{3}{2}, \frac{1}{2}, 1; x^2\right) + \frac{x^2}{2} F\left(\frac{3}{2}, \frac{3}{2}, 2; x^2\right), \quad (28)$$

$$G_2(x) = F\left(\frac{1}{2}, \frac{3}{2}, 2; x^2\right) + \frac{x^2}{2} F\left(\frac{3}{2}, \frac{5}{2}, 3; x^2\right), \quad (29)$$

where F is the hypergeometric function. Because we are dealing with two symmetric confocal domains, we can express the surface, volume and energy of the cyclides under closed form as

$$\frac{S}{8\pi^2} = \frac{b^2 r}{a} G_1\left(\frac{c}{a}\right), \quad (30)$$

$$\frac{V}{4\pi^2} = \frac{b^2 r^2}{a} G_1\left(\frac{c}{a}\right) + \frac{b^2 c^2}{2a} G_2\left(\frac{c}{a}\right), \quad (31)$$

$$\frac{2E}{\pi^2} = \frac{R^2}{R_1(R^2 - R_1^2)^{\frac{1}{2}}} - c_0 \frac{S}{\pi^2 r} + c_0^2 \frac{S}{\pi^2}, \quad (32)$$

and figure 6 gives the corresponding reduced volume drawn as a function of eccentricity.

It appears that the lowest reduced volume torus corresponds to the axisymmetric case. This observation may be relevant to experiments since partially polymerized vesicles reach their equilibrium shape after an inflation stage. The axisymmetric torus is, therefore, the first equilibrium shape accessible to the system.

Let us define $x = \frac{c}{a}$ as the scaled eccentricity. In order to keep a constant area and a constant volume as one moves the hole off the center by an amount of x , one has to choose the breathing amplitude $r(x)$ and the scale $a(x)$ as

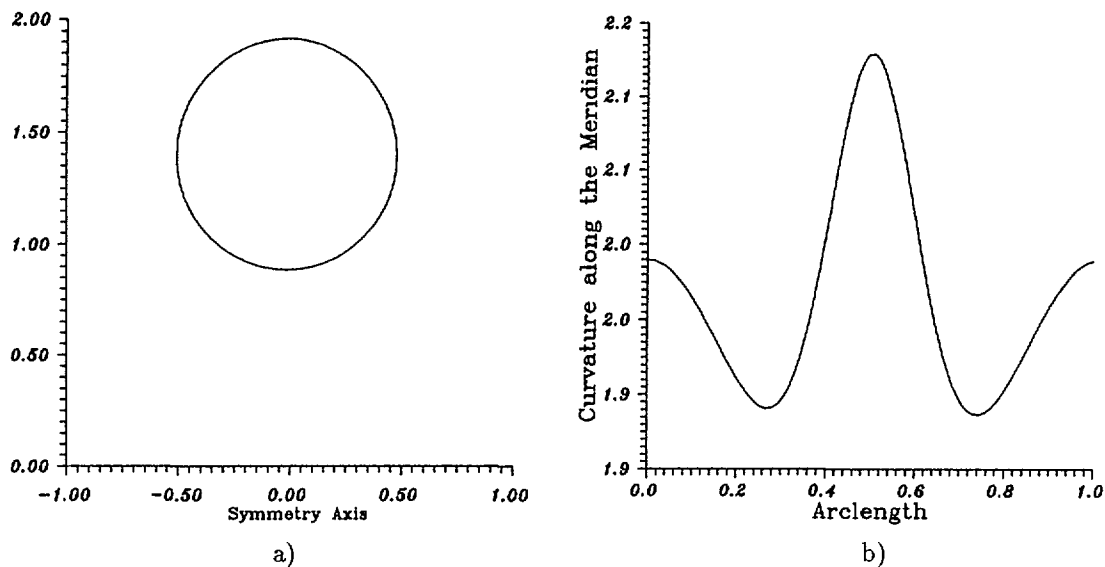


Fig.7. — Numerical axisymmetric solution of an almost circular torus. Part a: Meridian cross-section. Part b: variation of the curvature as one moves anti-clockwise from the equator.

$$r(x) = \frac{\sqrt{2}}{a(x)G_1(x)(1-x^2)\delta^{\frac{1}{2}}}, \quad (33)$$

$$a(x) = \frac{\delta}{G_2(x)x^2(1-x^2)} \left(1 - (1 - 4x^2 \frac{G_2(x)}{G_1(x)} \delta^{-2})^{\frac{1}{2}} \right), \quad (34)$$

with $b = a(x)\sqrt{1-x^2}$. In equation (33) the surface and the volume are normalized as $S = 4\pi^2\sqrt{2}$ and $V = 4\pi^2\delta$, respectively.

This variational Ansatz can be tested with respect to exact numerical solutions in the axisymmetric case. Seifert [8] has shown that the lowest energy stationary axis-symmetric shapes are almost circular when the reduced volume is closed to the value of the Clifford Torus. Figure 7 shows one of these solutions, where the curvature across the meridian varies within 10 % of its mean value. For $c_0=1$, this solution has an energy of 0.500 ± 5 which compares well with the energy of a variational and circular torus of the same volume and surface for which one gets: $E = 0.501$.

4.2 PHYSICAL CONSEQUENCES. — Let us begin with the zero spontaneous case, where an experimentally accessible quantity can be read off from the above parameterization. The experiment we have in mind consists in changing the reduced volume v of an axis-symmetric Clifford torus by means, for example, of a change in osmotic pressure.

As the reduced volume decreases, the hole moves off the center and the diameter of its circular shape is a function of its eccentricity. Since the hole is centred on the focal point at a distance c from the origin, its radius is $R = a - r$. To obtain scale invariant quantities, we set $a = 1$ and the relative radius R depends on its eccentricity c as (see Fig. 5 for geometrical definitions)

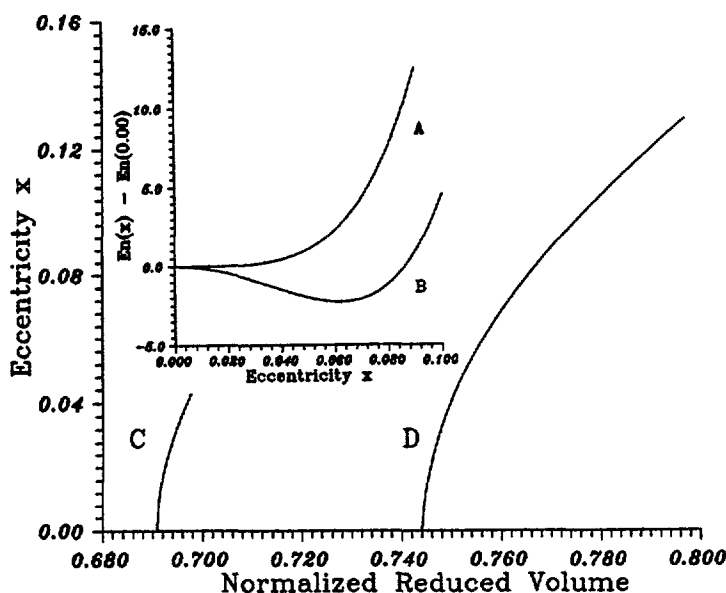


Fig.8. — Eccentricity x for the Dupin variational Ansatz as a function of $\frac{v}{v_{\text{Clifford}}}$. All curves have been drawn for $c_0 = 1$. Case C corresponds to the constant area problem of section 4.2. Curve D corresponds to the constant volume problem. Inset: Energy as a function of the eccentricity (normalized by 10^3) for the constant area problem. Curve A corresponds to $v = v_{\text{crit.}} = 0.691... v_{\text{Clifford}}$ and Curve B to $v = 0.705... v_{\text{Clifford}}$.

$$R = 1 - \sqrt{\frac{1+c^2}{2}} \quad (35)$$

Since for $c_0 > 0$, the equilibrium shape of the same reduced volume is non-axi-symmetric, the problem is to know the critical reduced volume at which the instability occurs. Because the spontaneous curvature sets a scale in the problem, $v_{\text{crit.}}$ is not the same when one increases the reduced volume with the surface kept constant, or when the reduced volume is increased with keeping a constant volume. We shall see, however, that the respective thresholds for the instability are almost identical. Figure 8 summarizes our results. Below a critical reduced volume smaller than the Clifford one, the shape is axi-symmetric and above this threshold, the minimum energy shape has a non-zero eccentricity. It should be, however, noted that the absolute minimum is axi-symmetric.

We first consider the case of a fixed surface equal to $4\pi^2\sqrt{2}$. This situation corresponds, for example, to a deflation of the vesicle, driven by a change in osmotic pressure. Using the variational Ansatz of the previous section, one can compute the energy as a function of the reduced volume $v = v_{\text{Clifford}}(1 + \epsilon)$. For $\epsilon \ll 1$ and to second order in the eccentricity of the hole, $x = \frac{c}{a}$, one finds that the energy behaves as

$$\frac{2E}{\pi^2} = 2 - 4c_0\sqrt{2}(1 - \epsilon) - 4x^2((9 - 3c_0\sqrt{2})\epsilon + c_0\sqrt{2}) + 4c_0^2\sqrt{2}. \quad (36)$$

For $\epsilon = 0$, one recovers the stability analysis of the previous section, since the first mode, $\delta\psi_{1,0} = a_1 \cos(\phi)$ moves the hole by $\eta_0 a_1$. However, when the reduced volume decreases below

$$v_{\text{crit.}}(S = \text{cst.}) = \left(1 - \frac{c_0\sqrt{2}}{9 - 3c_0\sqrt{2}}\right) v_{\text{Clifford}}, \quad (37)$$

the circular axisymmetric torus is the lowest energy state. For small spontaneous curvature, the circular approximation should be valid and the *actual absolute* minimum should correspond to an axisymmetric torus with a slight elliptical deformation of its meridian cross-section.

Consider now a problem where the volume is kept constant. Because the thermal expansion of the lipidic bilayer is much larger than the thermal expansion of the inside solution, this case could correspond to an experiment where the temperature of the vesicle is increased. A similar calculation as before for a torus of volume $4\pi^2$ gives

$$\frac{2E}{\pi^2} = 2 - 4c_0\sqrt{2}\left(1 - \frac{4}{3}\epsilon\right) - 4x^2\left(\left(9 - \frac{8}{3}c_0\sqrt{2}\right)\epsilon + c_0\sqrt{2}\right) + 4c_0^2\left(1 - \frac{2}{3}\epsilon\right)\sqrt{2}, \quad (38)$$

with a critical reduced volume

$$v_{\text{crit.}}(V = \text{cst.}) = \left(1 - \frac{c_0\sqrt{2}}{9 - \frac{8c_0}{3}\sqrt{2}}\right) v_{\text{Clifford}}, \quad (39)$$

so that the threshold is identical to the constant volume problem to first order in c_0 . However, for large eccentricity, the two energies will differ [22].

The conclusion of this section is that the spontaneous curvature selects one of these non-axisymmetric shapes when the reduced volume is large enough. Our presentation follows the usual Landau formalism for a phase transition with broken symmetry. Because we take the reduced volume as the control parameter, we find that the eccentricity behaves as

$$x \sim (v - v_{\text{crit.}}(c_0))^{\frac{1}{2}},$$

and is a linear function of the spontaneous curvature.

5. Conclusion.

The theoretical results of this paper have been motivated by recent experimental findings on vesicles of toroidal topology. An important aspect of these experiments is that the vesicles are polymerized in the gel state. When the system is reheated above the chain melting transition, there is an inflation stage and the generic toroidal vesicle corresponds to the Clifford torus or to a small subset of its conformal transforms. Because polymerization is below percolation threshold, it is natural to assume that the shape of the vesicle is controlled by a bending Hamiltonian. Although the microscopic mechanisms which select the toroidal topology are not yet controlled [23], it seems that these systems *adjust* their constraints to sit at the absolute minimum of the curvature energy.

This contrasts with usual liquid vesicles where the system minimizes its energy *given* the constraints. The physical mechanism which changes the rules of the game can be dynamic: If the kinetics which controls the plugging of the pores during the inflation stage is sufficiently slow with respect to the typical equilibration time scale, the system can finally sit at the absolute minimum. On a longer time scale, however, the holes are plugged because of the very high line tension associated with an aperture. Therefore, on this long time scale, the system is subject to the constraints of constant volume and area and the system is locked at a given fixed reduced volume. The conformal mode of Duplantier [7] is no more a zero-energy mode (see the Dupin cyclides section) and the constraints select one of the conformal transforms

of the Clifford torus. How many of the results presented in this paper apply to this physical situation ?

From the Willmore conjecture, it is clear that the equilibrium shape corresponds to the Clifford torus. What we can learn from the stability analysis is how the constraints affect the conformal mode of Duplantier [7]. In the zero spontaneous curvature case, we have found that the constraints of constant surface and of constant volume do not change this Goldstone mode picture when the stability analysis is pushed to second order. As a result, it is likely that the hole shows large thermal fluctuations around its equilibrium position since the energy is fourth order in the eccentricity of the hole. This is in contrast with other symmetry breaking modes which obey Hookes law.

We have also considered the effect of a small spontaneous curvature. The main consequence is that it selects a large branch of non-axi-symmetric tori. The variational Ansatz has, moreover, shown that the absolute minimum is still axi-symmetric and that it corresponds to the lowest reduced volume.

The application of a small spontaneous curvature model to partially polymerized membranes needs, however, a comment. In the laboratory, polymerization is done in a highly curved state so that the polymerized patches immersed in the fluid vesicle retain their wisped shape. The contiguous liquid lipid molecules must match these curved polymerized domains and this may result in effective induced curvature. The sign of this spontaneous curvature depends, however, on the distribution of patches and can be vesicle dependent.

Figure 4 clearly shows how the axi-symmetric Clifford torus can be unstable with respect to a shift of the hole when the spontaneous curvature is positive. Our proposal is to study how the hole shrinks as it moves off the center, see equation (35). Although a spontaneous curvature may be controlled in the laboratory by changing the electrostatic properties of the aqueous solution, there are a number of experiments which may lead to the same effect. This can also be done mechanically by changing the osmotic pressure: if the vesicle inflates, the reduced volume increases and the experimental path corresponds to figure 6.

The same experiment could be performed by increasing the temperature. Because the thermal expansion of the bilayer is much larger than that of the aqueous solution, this amounts to an effective change of area. The two leaflets of the bilayer may have, however, different thermal expansions and this property has been useful for the budding problem [24]. We point out that a differential change of the areas of the two leaflets lead necessarily to a frustration effect when the lipidic chains reach their maximum extension [25]. Since it costs a lot of energy to change by a small amount the intra-bilayer volume, the hole will stick to a maximum eccentricity. In this case, frustration can only be resolved by introducing topological defects and by tearing one of the leaflets. Farge and Devaux [26] have shown that a pH-induced flip-flop mechanism between the two leaflets of the bilayer may be a more effective mechanism to monitor a differential area change.

The challenge is to look at high genus surfaces. Reference [1] has already demonstrated that they are experimentally observable. Since the shape of the two-holed torus is highly symmetric, one can suspect that this example also has an extremal reduced volume for small perturbations around its equilibrium shape, as the axi-symmetric Clifford torus does. From the lore of mathematics [10], one expects a rich variety of shapes: Lawson N-holed tori or even Klein bottles. In the spirit of this discussion, the problem is to know which one has the lowest reduced volume [27].

Acknowledgments.

I wish to acknowledge particularly D. Bensimon and M. Mutz for kindly introducing me to the physics of partially polymerized membranes. I would also like to thank B. Duplantier for sharing freely his insights. Finally I would like to acknowledge J. Charvolin, P. Nozières, J. Chalker, U. Seifert and M. Wortis for numerous and useful discussions. The kind hospitality of the Physics department of Simon Fraser University, where part of this work has been done, is also gratefully acknowledged.

Appendix A.

Some formulae for toroidal surfaces.

We recall that tori with a circular meridian cross-section are $\eta = \text{cst}$ surfaces with

$$x = \frac{\sinh(\eta) \cos(\phi)}{\cosh(\eta) - \cos(\theta)}; \quad (\text{A.1})$$

$$y = \frac{\sinh(\eta) \sin(\phi)}{\cosh(\eta) - \cos(\theta)}; \quad (\text{A.2})$$

$$z = \frac{\sin(\theta)}{\cosh(\eta) - \cos(\theta)}. \quad (\text{A.3})$$

In the general case of a $\eta(\theta, \phi)$ surface, the metric tensor gives the area as

$$S = \int_0^{2\pi} \int_0^{2\pi} d\theta d\phi \sqrt{g}, \quad (\text{A.4})$$

with

$$g = \frac{\sinh(\eta)^2}{(\cosh(\eta) - \cos(\theta))^4} \left(1 + \left[\frac{1}{\sinh(\eta)^2} \left(\frac{\partial \eta}{\partial \phi} \right)^2 + \left(\frac{\partial \eta}{\partial \theta} \right)^2 \right] \right). \quad (\text{A.5})$$

The volume enclosed by the surface is simply obtained as

$$V = \int_0^{2\pi} d\phi \int_0^{2\pi} d\theta \int_{-\infty}^{\eta(\theta, \phi)} d\eta \sqrt{g} \quad (\text{A.6})$$

To perform all the integrals we have found it useful to replace the toroidal angle θ by the cylindrical angle $\bar{\theta}$ giving the usual parameterization of a torus. Both are related by

$$\sin(\bar{\theta}) = \frac{\sinh(\eta) \sin(\theta)}{\cosh(\eta) - \cos(\theta)} \quad (\text{A.7})$$

$$\cos(\bar{\theta}) = \frac{\cosh(\eta) \cos(\theta) - 1}{\cosh(\eta) - \cos(\theta)}, \quad (\text{A.8})$$

and all integrals can be done by using one of the formulae

$$\int_0^{2\pi} d\theta \frac{(\cosh(\eta) + 2 \cos(\theta))^2}{\cosh(\eta) - \cos(\theta)} = 2\pi \frac{\cosh(\eta)^2}{\sinh(\eta)}; \quad (\text{A.9})$$

$$\int_0^{2\pi} d\theta \frac{\cosh(\eta) + 2 \cos(\theta)}{\cosh(\eta) - \cos(\theta)} = 2\pi \frac{2 \sinh(\eta) - \cosh(\eta)}{\sinh(\eta)}; \quad (\text{A.10})$$

$$\int_0^{2\pi} d\theta \frac{1}{\cosh(\eta) - \cos(\theta)} = \frac{2\pi}{\sinh(\eta)}. \quad (\text{A.11})$$

References

- [1] Deuling H.J. and Helfrich W., *J. Phys. France* **37** (1976) 1335;
Svetina S.V. and Žekš, *Biomed. Biochem. Acta* **42** S86 (1983);
Berndl K., Käs J., Lipowsky R., Sackmann E. and Seifert U., *Europhys. Lett.* **13** (1990) 659;
Miao L., Fourcade B., Rao M., Wortis M. and Zia R.K.P., *Phys. Rev. A* **43**, (1991) 6843;
Seifert U., Berndl K. and Lipowsky R., *Phys. Rev. A* **44** (1991) 1182;
Lipowsky R., *Nature* **349** (1991) 475.
- [2] Fourcade B., Bensimon D. and Mutz M. *Phys. Rev. Lett.* **68** (1992) 2551.
- [3] Mutz M. and Bensimon D., *Phys. Rev. A* **45** (1991) 4525;
Mutz M. and Bensimon D., in Proceedings of the workshop on Dynamical Phenomena at Interfaces, Surfaces and Membranes (Les Houches 1991) to appear.
- [4] Canham P.B., *J. Theor. Biol.* **26** (1970) 61;
Helfrich W., *Z. Naturforschung* **28 c** (1973) 693;
Evans E.A., *Biophys. J.* **30** (1980) 265.
- [5] Willmore T.J., *Total Curvature in Riemannian Geometry*, (Ellis Horwood Ltd., Chichester, 1982).
- [6] Ou-Yang Zhong-Can, *Phys. Rev. A* **41** (1990) 4517.
- [7] Duplantier B., *Physica (Amsterdam)* **168A** (1990) 179.
- [8] Seifert U., *Phys. Rev. Lett.* **66** (1991) 2404.
- [9] Seifert U., *J. Phys. A* **24** (1991) L573.
- [10] Pinkall U. and Sterling I., *Math. Intelligencer* **9** (1987) 38;
Lawson H.B., Jr., *Ann. Math.* **92** (1970) 335;
Karcher H., Pinkall U. and Sterling I., M.P.I. 86-27 preprint.
- [11] Peterson M.A., *Phys. Rev. Lett.* **61** (1988) 1325.
- [12] By definition, the mean curvature is positive on the outside of the torus but negative on the leaf surrounding the hole.
- [13] Hilbert D. and Cohn-Vossen S., *Geometry and Imagination* (Chelsea Pub. Cy., New York, 1970).
- [14] Kléman M., *J. Phys. France* **38** (1977) 1511;
Bouligand Y., *J. Phys. France* **33** (1972) 525.
- [15] If c_1 and c_2 are the two principal radii of curvature, this amounts to writing the bending energy as

$$\frac{1}{2} \int dS \left(\frac{1}{2} (c_1 + c_2) - c_0 \right)^2,$$

which differs by a factor $\frac{1}{2}$ from the convention chosen in reference [2], but agrees with the convention of reference [5]. The spontaneous curvature c_0 is introduced in section 3.

- [16] The mapping from S^3 to R^3 for a torus is also described in (without the surface and volume constraints) : Mosseri R., Sadoc J.F. and Charvolin J., *Amphiphilic Membranes*, R. Lipowsky Eds., Springer Proceedings in Physics, to be published.
- [17] The same property holds for any mappings in arbitrary dimension, see reference [5] for a discussion on this point.

- [18] The Goldstone phenomenon has been previously studied by Peterson M.A. for the case of a quasi-spherical vesicle: See Peterson M.A., *Mol. Cryst. Liq. Cryst.* **127** (1985) 257.
- [19] The electrostatic problem has been calculated by Duplantier B., Goldstein R.E., Romero-Rochin V. and Pesci A.I., *Phys. Rev. Lett.* **65** (1990) 508.
- [20] We point out that the pdV term is crucial to obtain the same result for the constant area - constant volume ensemble and constant pressure - constant volume ensemble. Without this term, we find that the bare energy is

$$-\frac{3}{2}(1+c_0\sqrt{2})a_n^2n^2+a_n^2(1+\frac{3}{2})4\sqrt{2}c_0+\frac{1}{2}a_n^2n^4,$$

when there is a coupling with a rescaling to keep a constant surface. However, if one uses a breathing mode to satisfy this constraint, one finds

$$-(\frac{3}{2}+\frac{5\sqrt{2}}{3}c_0)a_n^2n^2+a_n^2(1+\frac{\sqrt{2}}{3}c_0)+\frac{1}{2}a_n^2n^4.$$

- [21] The operator Δ corresponds to the Laplace-Beltrami operator defined as

$$\frac{1}{\sqrt{\det(g)}}\partial_i\sqrt{g}g^{ij}\partial_j.$$

It may be useful to note that, for finite spontaneous curvature, the axi-symmetric Clifford torus is the *only* Dupin Cyclide with a circular meridian cross-section which is solution of the Euler-Lagrange equations.

- [22] A numerical minimization procedure for $c_0 = 1$ shows that the critical volume ratios are $v_{\text{crit.}}(S = \text{cst}) = 0.691$ and $v_{\text{crit.}}(V = \text{cst}) = 0.744$, respectively. To first order in $v - v_{\text{Clifford}}$, they agree with equations (37) and (39).
- [23] A reasonable hypothesis is that the topology is selected by defects when the lamellae close and form a vesicle.
- [24] See Berndt K. et al. and Seifert et al. in reference. [1].
- [25] The concept of frustration for two parallel interfaces at a constant distance has been introduced by Charvolin and Sadoc. For a reference, see Charvolin J. and Sadoc J.F., *J. Chem. Phys.* **92** (1990) 5787.
- [26] Farge E. and Devaux F., to appear in *Eur. Biophys. J.*
- [27] It seems that the minimal reduced volume problem has also been considered in Mathematics, see chapter 6 of reference [5].